

Colour gradients within SDSS DR7 galaxies: Hints of recent evolution

V. Gonzalez-Perez^{1,2}, F. J. Castander², G. Kauffmann³

¹*Institute for Computational Cosmology, Department of Physics, University of Durham, South Road, Durham, DH1 3LE, UK*

²*Institut de Ciències de l'Espai (CSIC/IEEC), F. de Ciències, Torre C5 Par 2a, UAB, Bellaterra, 08193 Barcelona, Spain*

³*Max-Planck Institut für Astrophysik, D-85741 Garching, Germany*

1 June 2019

ABSTRACT

The evolutionary path followed by a galaxy shapes its internal structure, and, in particular, its internal colour variation. We present a study of the internal colour variation within galaxies from the Seventh Data Release of the Sloan Digital Sky Survey (SDSS DR7). We statistically study the connection between the internal colour variation and global galactic properties, looking for hints of the galactic recent evolution. Considering only galaxies with good photometry and spectral measurements, we define four luminosity-threshold samples within the redshift range $0.01 < z < 0.17$, each containing more than 48000 galaxies. Colour gradients are calculated for these galaxies from the surface brightness measurements provided by the SDSS DR7. Possible systematic effects in their determination have been analysed. We find that, on average, galaxies have redder cores than their external parts. We also find that it is more likely to find steep colour gradients among late-type galaxies. This result holds for a range of classifications based on both morphological and spectral characteristics. In fact, our results relate, on average, steep colour gradients to a higher presence of young stars within a galaxy. Our results also suggest that nuclear activity is a marginal driver for creating steep colour gradients in massive galaxies. We have selected pairs of interacting galaxies, with a separation of $5''$, in projected radius, and a difference in redshift of 100 km/s , finding that they present steeper gradients than the average population, skewed towards bluer cores. Despite the large dispersion in colour gradient values, this parameter can be useful for selecting galaxies that have suffered a recent (minor) burst of star formation.

Key words: galaxies: fundamental parameters, statistics, structure

1 INTRODUCTION

The subtleties of galaxy formation remain to be understood. The study of the internal structure of galaxies can help us to understand how they formed and evolved. Here we study the internal colour variation across galaxies, quantified through their colour gradient. Interest in internal colour variation has grown enormously in the last five years, especially due to the availability of both shallow large surveys such as the Sloan Digital Sky Survey (SDSS, York et al. 2000), that can provide statistically significant samples of galaxies, and deep surveys, such as those performed with the Hubble Space Telescope (HST; (e.g. Menanteau et al. 2005; Ferreras et al. 2009)), that provide high resolution images of galaxies at $z > 0.5$. Previous work has used the colour gradient as a measure of the galactic internal colour variation, which has proved to be very useful for exploring galactic properties (e.g. Wu et al. 2005), due to its tight dependency on the galactic distribution of metallicity, stellar age and dust (see e.g. Michard 2005; Rawle et al. 2010; Tortora et al. 2010). This, together with the accessibility of gradient measurements, since only photometry is needed, makes the colour gradient a useful tool to obtain statistical results for wide samples

of galaxies, that will be interesting to relate to different theoretical aspects from models of galaxy formation.

In general, galaxies tend to have cores that are redder than their external parts (e.g. Peletier et al. 1990). In this work we study the variation within nearby galaxies of the following optical colours: $(g-i)$, $(g-r)$, $(r-i)$, $(i-z)$ and $(r-z)$. Both $(g-r)$ and $(g-i)$ rest frame colours are most sensitive to the intensity of the spectral break that appears around 4000 \AA , due to the accumulation of resonant absorption lines from metals in different stages of ionisation (e.g. Hamilton 1985). This break correlates with the temperature of the dominant stellar population, increasing for cooler stars, but it does not depend strongly on the galactic metallicity. Unlike late-type galaxies, early-type ones are dominated by K-type stars, showing a rather steep change in flux from g to r or i -band. If we consider that these colours are mainly related to the age of the galaxy then the redder core will imply that it is also older.

The other three colours, $(r-i)$, $(r-z)$ and $(i-z)$, in the rest frame directly depend on the proportion of main sequence to red giant branch or older stars (Bruzual and Charlot 1993). Thus, we could simply record these colours as depending on the relative

amount of old and young stars in the galaxies, though this is less clear for $(i - z)$ and has a smaller dynamic range in the case of the $(r - i)$ colour. Thus, we observe the same tendency as before: redder cores imply that in general galaxies tend to have older stars in their centres.

However, these implications should be taken with caution both because global colours can be affected by marginal young populations (Li and Han 2007) and because colours within different galactic annuli do not agree well with global ones. Besides, broad band colours show a degeneracy in their dependence with stellar population age and metallicity (e.g. Worthey 1994; Charlot, Worthey & Charlot 1996). Indeed, several studies (see e.g. Tamura & Ohta 2004; Wu et al. 2005; Barbera et al. 2009; Tortora et al. 2010) have shown that metallicity and not age gradients are the principal origin of colour variation. In the case of early-type galaxies, age gradients have been measured to be almost flat or positive while metallicity gradients are negative, i.e. early-type galaxies tend to have younger, higher metallicity cores (see e.g. Sánchez-Blázquez et al. 2006; Rawle et al. 2010). Late-types are more complex, showing a broad variety of age and also metallicity gradients, due to the interplay between dust content, stellar feedback, bursts of formation and stellar migration due to the instabilities that trigger the formation of bars but also the spiral arms. MacArthur et al. (2009) observed that spiral galaxies have bulges with positive age gradients, while their disks show negative ones, but there are examples of spiral galaxies with negative age gradients for most of their extension, except for the most external radii (Vlajić et al. 2009).

Metallicity gradients within galaxies can be produced through different mechanisms. Winds generated by supernovae (Larson 1974) or active galactic nuclei (AGN) (Begelman, de Kool and Sikora 1991) can provide the metallicity enrichment of the inter stellar or even the inter galactic medium. Due to the multiple phases that compose this medium the enrichment does not necessary happen in a symmetrical way, which can produce strong metallicity gradients and thus colour gradients. Galaxies with a significant age gradient can present very shallow or even inverted colour gradients (Hinkley & Im 2001), since age gradients usually arise from localised regions of star formation, generally resulting in galaxies with bluer cores than their external parts. The presence of a diffuse component of dust could also explain some colour gradients. However, this has a marginal impact, specially for early-type galaxies, which are almost dust free (Michard 2005; Wu et al. 2005). In summary, colour gradients in galaxies are likely to be related to the different star formation histories followed, which depend on the way gas is distributed and collapses after accretion and mergers.

Many studies of colour gradients try to clarify the dependence on the star formation history of galaxies. This aspect is of particular interest since it could help us to understand how galaxies form and evolve. The recent study by Suh et al. (2010) of early-type galaxies drawn from the SDSS DR6 reports a tight correlation between the existence of steep colour gradients and ongoing residual star formation. This study of galaxies at $z < 0.06$ suggests a relation between elliptical galaxies with bluer cores presenting global bluer colours than average. Ferreras et al. (2009) found the same relation for spheroidal galaxies observed by the HST at $0.4 < z < 1.5$. Lee et al. (2008) found that steeper colour gradients appear within star forming galaxies, in both late and early-types. A similar result was found in the recent study by Tortora et al. (2010), where older galaxies are observed to have systematically shallower age and metallicity gradients, and thus, colour gradients. The colour gra-

dients of spiral galaxies appear to be dominated by the fact that, on average, their bulges are redder than their disks. However, this is an oversimplification for many late-type galaxies (see e.g. Bakos et al. 2008).

Cosmological simulations do not yet have sufficient resolution to make predictions for colour gradients. However, semi-analytical models which include a bulge-disk decomposition and spatially resolved star formation, could provide some useful insight for this particular problem (Stringer & Benson 2007). Nevertheless, in general, gas-dynamical simulations with high enough resolution to follow physical processes within galaxies are needed in order to produce theoretical predictions for the internal characteristics of galaxies. “Monolithic collapse” models can produce elliptical galaxies with colour gradients that agree with observations if a certain scatter is allowed for the star formation efficiency (Pipino et al. 2010). These monolithic models also predict steeper gradients for more massive galaxies, something that is observed up to $M_* \sim 3.5 \times 10^{10} M_\odot$ (Spolaor et al. 2009; Rawle et al. 2010; Tortora et al. 2010). For more massive galaxies, the contribution of mergers provides a larger scatter that smears out such correlation. Kobayashi (2004) used chemo-dynamical simulations of merging galaxies to understand elliptical galaxy formation. The resultant galaxies had metallicity gradients consistent with observations. The predicted gradients depend strongly on the relative properties of the progenitor galaxies, i.e., on the particular formation process of a galaxy.

In this paper, we study the largest data set to date, which allows us to make a statistically robust analysis of the internal colour variation within nearby galaxies. We study four luminosity-threshold samples, defined in section §2. We obtain colour gradients directly from the SDSS photometric data and we (K+e) correct global magnitudes using spectral energy distributions (SEDs) generated with PEGASE (Fioc & Rocca-Volmerange 1997). This process is described in section §2.1. In section §3 we analyse the colour gradients distribution and we also study the possible correlations between the colour gradient and global galactic properties, including galactic types and redshift. Finally we summarise our results and conclusions in section §4.

In this study we use Petrosian magnitudes for setting the sample limits. Apparent magnitudes are corrected from the extinction due to our galaxy, but not to their internal reddening. Model magnitudes are used only for global galactic colours. All magnitudes used in this paper are in the AB system, unless otherwise specified. We assume a flat cosmology, $\Omega_k = 0$, with a critical matter density of $\Omega_m = 0.3$ and a Hubble constant, $H_0 = 100 \text{ h km s}^{-1} \text{ Mpc}^{-1}$ with $h = 0.7$ (Spergel et al. 2003).

2 THE DATA

Our sample is drawn from the SDSS DR7 (Abazajian et al. 2009) spectroscopic main galaxy targets. The SDSS DR7 has covered spectroscopically an area of 9380 deg^2 , providing a redshift accuracy of 30 km/s rms for the main galaxy sample. The SDSS main spectroscopic sample is described by Strauss et al. (2002). Galaxies within this sample have $r < 17.77$ (Petrosian magnitude after correcting for galactic extinction) and a median redshift of $z \sim 0.1$.

From the SDSS main spectroscopic sample, we further select those galaxies that, according to the SDSS pipeline flags, have a reliable determination of their redshift, a good photometry¹ in all

¹ By good photometry we mean here that according to the SDSS pipeline

g, r, i and z bands, have a good determination of their Petrosian radius and a complete surface brightness profile measurement. In order to avoid those galaxies most affected by aperture effects, a lower limit to the galaxy redshift has been imposed, $z > 0.01$.

After applying the above restrictions we found that one of the galaxies appeared multiple times due to different deblending of objects at successive scans. After taking out this galaxy our initial sample contains 339711 galaxies.

As it will be detailed in §2.3 we quantify the internal colour variation using the SDSS DR7 measurements of surface brightness averaged within circular concentric annuli. At most there are 15 measurements, though, in most cases there are less due to the low surface brightness of many galaxies. The outer radii of these annuli are fixed and range from 0.22" to 258.38", growing approximately exponentially².

We make use of the stellar masses, star formation rates, some spectral indices and classification provided in the SDSS MPA/JHU³ collaboration database (Kauffmann et al. 2003a; Brinchmann et al. 2004), which has been updated for the SDSS DR7. These parameters are obtained by extrapolating to the full galaxy the spectroscopic information collected within the 3" diameter fibre set around the galactic centres. The extrapolation is done taking into account the global galactic colour and the effects due to dust. This extrapolation does not consider the colour gradients within galaxies, which could include a systematic effect on the determination of global properties.

2.1 (K+e)-correction

The (K+e)-correction accounts for two effects. One, the K-correction, is the shift of the filter in the galaxy's rest frame with redshift due to observing with a fixed band (Oke & Sandage 1968). The other, the e-correction, accounts for the change in luminosity due to ageing of existing stellar populations or new star formation that galaxies experience up to $z = 0$ from the epoch at which they are observed (Poggianti 1997). Both effects vary between the different bands. Within the SDSS bands we obtain larger corrections for bluer bands (Fukugita et al. 1995). In order to make sure that we are comparing similar spectral regions from different galaxies we need to apply the (K+e)-correction.

The (K+e)-correction is evaluated fitting the galaxy photometry to the best model within a grid of SEDs generated with the population synthesis models PEGASE (Fioc & Rocca-Volmerange 1997). The grid is made using the default template SEDs produced within PEGASE, matching the colours observed for different Hubble galactic types at $z \sim 0$, and includes a galaxy formed in a 1Gyr long burst, an elliptical and a lenticular galaxies, spiral galaxies: Sa, Sb, Sbc, Sc, Sd and three irregular galaxies with different formation redshifts.

There are six galaxies in our initial sample with colours that are not well fitted by the synthetic ones. These are left out of the

flags the galaxies are detected at more than 5σ level, with all their pixels checked for possible centres, not being a blended object, without too many interpolated pixels, without pixels hit by a cosmic ray and without a faulty sky subtraction.

² For further details we refer the reader to the SDSS help page <http://cas.sdss.org/dr7/en/help/browser/constants.asp?n=ProfileDefs> and the document on profiles written by R. Lupton & J. Gunn: <http://www.astro.princeton.edu/~rhl/photomisc/profiles.ps>

³ <http://www.mpa-garching.mpg.de/SDSS/>.

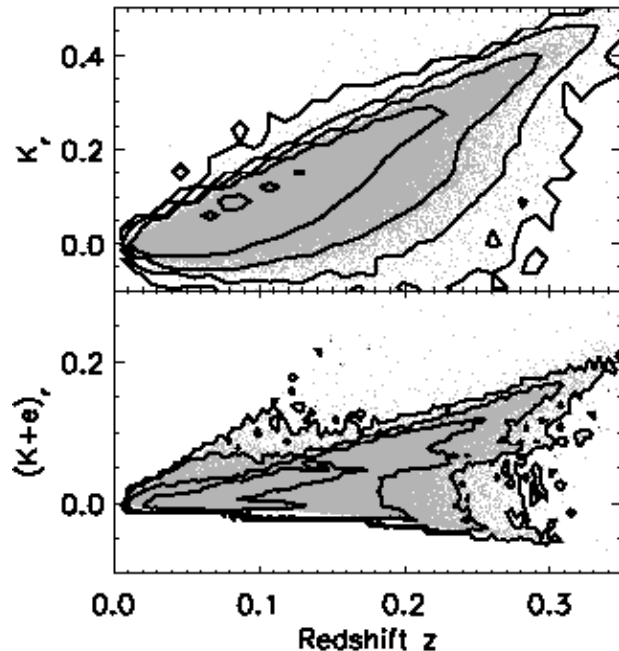


Figure 1. K correction (top) and (K+e) correction (bottom) in the r-band as a function of redshift estimated by fitting PEGASE stellar population models to SDSS DR7 galaxy photometry. Contour levels represent an increase of a factor of ten and they are plot over single galaxy data points.

sample. Since these objects represent 0.002% of the sample we do not apply any correction for their omission.

Both K and (K+e) corrections are shown in Fig. 1 for all galaxies in our initial sample. These corrections are applied to the global colours of galaxies in our sample. The K-correction alone tends to be larger for higher redshifts, but the dispersion increases at the same time. This behaviour has been found in other works (see e.g. Blanton et al. 2003; Fukugita et al. 1995).

We can observe in Fig. 1 that the (K+e)-correction shows a weaker dependency on redshift than the K-correction. This was also found in previous studies, such as Poggianti (1997). The reason for this flattening is that as they evolve, a galaxy luminosity decreases until a new burst of star formation occurred and is superimposed to an already old stellar population.

We checked the possibility of calculating the (K+e)-correction individually for different galactic radii. In order to test this possibility we obtained magnitudes in circular concentric annuli for each galaxy, from the averaged surface brightness measured by the SDSS pipelines. However, colours in individual annuli are noisier than global ones and the fitting procedure basically fits noisy features that result in obtaining unrealistic SEDs for each annulus. Therefore, we obtain the global (K+e)-correction for each galaxy, which presumably is an average of the correction to different annuli. The use of an average (K+e)-correction could introduce spurious colour gradients. These are difficult to evaluate, since they depend on the intrinsic metallicity and age gradients of each galaxy, higher signal-to-noise data would be needed to properly compute these correction as a function of radius and evaluate the effect of observing different radii at a given projected annulus. Applying a global corrections implies that the resultant colour gradients would

Name	Absolute magnitude	Redshift	No. galaxies
<i>S19</i>	$M_r - 5\log h < -19.$	$0.01 < z < 0.072$	48728
<i>S20</i>	$M_r - 5\log h < -20.$	$0.01 < z < 0.111$	82838
<i>S20.5</i>	$M_r - 5\log h < -20.5$	$0.01 < z < 0.1375$	86818
<i>S21</i>	$M_r - 5\log h < -21.$	$0.01 < z < 0.169$	66177

Table 1. The given name, absolute magnitude range, redshift range and final number of galaxies to be studied within the defined luminosity-threshold samples.

not be affected, since we are only moving the zero point on the colour vs. radius relation. This implies that similar colour gradients will be found either applying the (K+e)-correction or only the K-correction. However, applying one or the other changes very slightly the defined luminosity-threshold samples, and has a definite impact on the global colours associated to each galaxy.

We will restrict our study to galaxies seen up to such a redshift that the (K+e)-corrections would not be large. Rather than the actual value of the (K+e)-correction, the problem resides in the higher spread among template SEDs found at higher redshifts, which can introduce larger errors in the estimated correction. For the majority of galaxies up to $z < 0.17$, the (K+e)-corrections is well below a value of 0.6 in the g, r, i and z-bands. For the same range, the K-correction stays below 0.8 in all bands. There is another reason for not considering galaxies at the highest redshifts covered by the survey. While the distribution of the K-correction is smooth, it is clear that our estimate of the (K+e)-correction start to be almost discretised for galaxies with $z \geq 0.25$. This effect is not present at $z < 0.17$. In order to correct galaxies at $z > 0.17$ we need to enhance our grid of model SEDs, including different formation redshifts for not only Irregular galaxies but for all the Hubble types included as templates. This change should be done carefully, in order to reproduce the observed fluxes of galaxies at different evolutionary stages.

Taking into account the two mentioned sources of uncertainty we will restrict our study to galaxies with $z < 0.17$.

2.2 The luminosity-threshold samples

We have divided our initial sample of galaxies with $z < 0.17$ into four luminosity-threshold samples. These samples, though well defined, are not volume limited since they miss a cut in redshift corresponding to the bright limit of the survey. Fig. 2 shows the boundaries of each sample superimposed on the distribution of the absolute magnitude versus redshift for all galaxies. Absolute magnitudes have been obtained from the (K+e)-corrected Petrosian magnitudes in the r-band. Table 1 summarises the characteristics of the luminosity-threshold samples. We will refer to each sample by their absolute magnitude cut, as indicated in the first column of Table 1.

We find that some of the galaxies within the *S21* sample have a half light radius $R50 < 0.7''$, i.e., inside the first two annuli with surface brightness measurements. As explained in §2.3 these two annuli are not considered in the calculation of the colour gradients. Thus, for those galaxies within the *S21* sample we will be calculating colour gradients with only the outer half of the galactic light. For this reason, we will concentrate on the other three samples at $z < 0.14$, and results from the *S21* sample will be considered with caution.

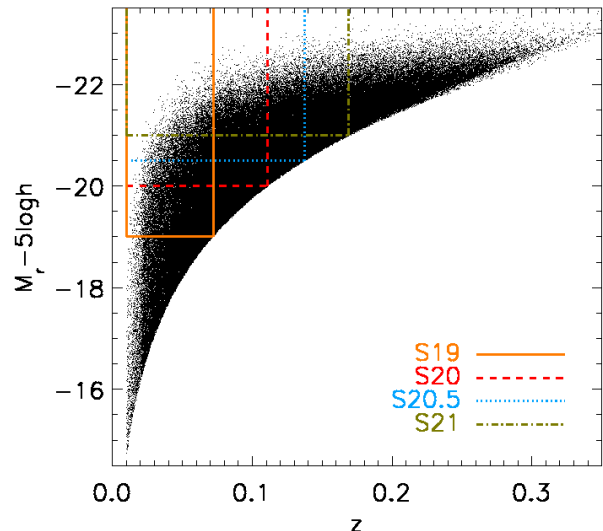


Figure 2. Redshift versus absolute magnitude in r band for the selected SDSS DR7 galaxies. The different luminosity-threshold samples are enclosed by solid lines for the *S19* sample, dashed for the *S20*, dotted for the *S20.5* and dash-dotted for the *S21*.

As explained in the next section §2.3, to obtain colour gradients, galaxies should have their surface brightness measured in at least four annuli, without considering the two innermost ones. Among our samples we find two galaxies which have their surface brightness measured in too few annuli, one within the sample *S20.5* and the other within the *S19* one. These two galaxies lack a colour gradient measurement and are not considered further.

As mentioned previously, we make use of some of the quantities derived from the SDSS database by the MPA/JHU collaboration. The cross identification using the position coordinates of the galaxies is not perfect. Fewer than 5% of those galaxies in our initial samples do not appear to have properties measured by the MPA/JHU collaboration. Only when using the MPA/JHU derived parameters we will be neglecting those galaxies.

2.3 Quantifying the internal colour variation through colour gradients

Different ways to compute the internal colour variation can be found in the literature. Some examples are: the slope of colour vs. normalised radius or its logarithm (e.g. Hinkley & Im 2001; Michard 2005; Tortora et al. 2010), the difference between colours outside and inside certain radius (e.g. Menanteau et al. 2005; Park & Choi 2005), the comparison between model and fibre colours when working with galaxies from the SDSS (e.g. Roche et al. 2009) and the colour variation averaged to all the pixels in an image (e.g. Menanteau et al. 2001).

In the early stages of this work we used the SDSS DR2 to estimate the best way to quantify the internal colour variation. We studied the internal colour variation within a sample of galaxies with a concentration index $C \geq 2.63$ and $z < 0.1$. The concentration index is defined as the ratio between two radii enclosing different amounts of light flux. The SDSS definition uses the radii containing 90%, $R90$, and 50%, $R50$, of the total galactic light. Strateva (2001) and Shimasaku (2001) found that $C = 2.6$ is the boundary that sep-

arates early from late-type galaxies, according to both their morphological and spectral features. The actual value of this boundary can vary depending on level of restriction needed for contaminants within one or the other type of galaxies

After thoroughly testing various methods using the quantities provided by the SDSS database, we reached the conclusion that the surface brightness profile appears to be the best way to quantify the internal colour variation in galaxies as opposed to magnitude based estimations, e.g. comparing the *fib*re or *PSF* colours with the global galactic colours.

The SDSS provides measurements of surface brightness averaged within circular concentric annuli at different galactic radii. We obtain colour gradients from these measurements. The two innermost annuli, $R < 0.7''$, are excluded from the calculation, since they are the most affected by seeing (the median PSF width in the r band for the SDSS DR7 is $1.4''$). Previous studies, such as that from Tamura & Ohta (2003) have reported that the internal colour variation is diminished if the annuli most affected by seeing are considered for obtaining the surface brightness profile.

From the SDSS averaged surface brightness profile we get the cumulative one. This last one is fitted to a taut spline⁴, using a fourth order polynomial. Thus we need galaxies to have measurements of average surface brightness in at least four annuli. The interpolated surface brightness points are differentiated. We then convert the resulting surface brightness into magnitudes. We do this last step only for the radii corresponding to the outer ones from the initial annuli. These magnitudes are corrected with the global (K+e)-correction obtained for the whole galaxy. Colour gradients are finally obtained by calculating the slope of the straight line that best fits the colours, $(m_1 - m_2)$, at different galactic radii (those for which a surface brightness profile is provided in the SDSS) versus the radii of the annuli normalised by the galaxy half light radius in the r -band, $R50$:

$$\nabla_{m_1 - m_2} = \frac{\Delta(m_1 - m_2)}{\Delta(R/R50)} \quad (1)$$

The normalisation in radius is done in order to allow us to compare galaxies with different light distributions and sizes.

When computing the errors on the measured gradients we use a Monte Carlo method to take into account the observational errors in both the surface brightness and $R50$ measurements. Surface brightness values within a galaxy are related, with one value influencing the values at outer radii. In order to simplify the calculation we use a compromise by effectively considering the surface brightness values as independent and restricting the random values, obtained with the Monte Carlo method, within 1σ . Thus, in order to include the observational errors, we repeat the whole process, except for the calculation of the (K+e)-correction, 1000 times for each galaxy using each time a random value extracted from the error distribution for the variables within 1σ of the measurements, assuming that the initial errors have a Gaussian distribution.

We obtain the probability distribution from the Monte Carlo

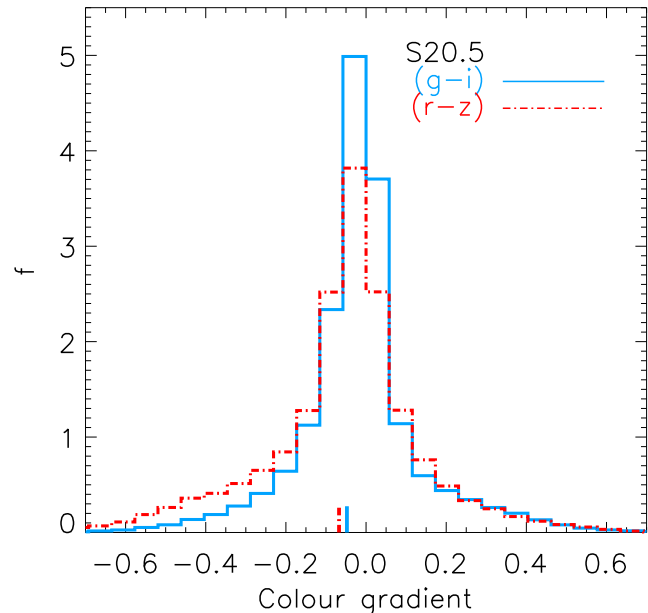


Figure 3. Distribution of $(g - i)$ (solid line) and $(r - z)$ (dot-dashed line) colour gradients for galaxies within the sample $S20.5$. Median colour gradient values are shown as short lines of the same type as their corresponding distribution. Histograms are normalised to give unit area underneath.

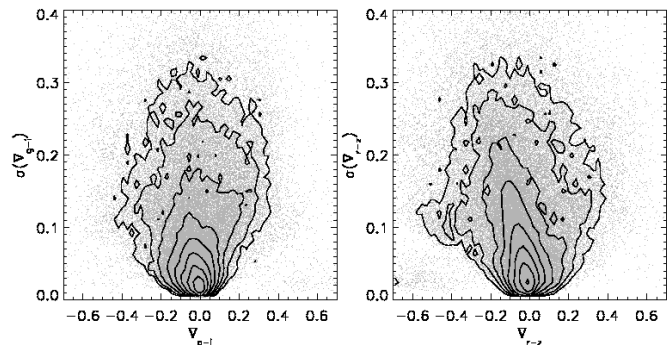


Figure 4. Distribution of colour gradients errors for $(g - i)$, (left) and $(r - z)$ (right) for galaxies in the $S20.5$ sample. Each contour represents a factor of two change in density.

runs making use of a *simple estimator*⁵ and then we calculate the expected value of the colour gradient and its variance.

3 RESULTS

Here we explore the origin of the colour gradient distribution in connection with the different classifications of galaxies into either early and late types or star forming, passively evolving and hosting nuclear activity.

⁵ The simple estimator, f , is basically a weighted histogram without a dependency on the selection of the first bin, though it maintains a dependency on the step size, h :

$$f(x) = \frac{1}{n} \sum_{i=1}^n \frac{1}{h} w \left(\frac{x - x_i}{h} \right) \quad (2)$$

Here the weight, w , is 0.5 if $|x - x_i| < 1$ and 0 otherwise.

⁴ A taut spline is a piecewise cubic interpolant for which the first and last internal knots are not used. See de Boor (1978) for a full description.

We have calculated the gradients for the $(g-i)$, $(g-r)$, $(r-i)$, $(i-z)$ and $(r-z)$ colours. Fig. 3 shows the distribution of the $(g-i)$ and $(r-z)$ colour gradients for galaxies in sample *S20.5*. We have found that the distributions of the colour gradients in the $(g-r)$ and $(g-i)$ colours are similar. The distributions of the colour gradients in the $(r-i)$, $(r-z)$ and $(i-z)$ colours are also similar between them. As described in the introduction this is due to the similarity in the spectral characteristics that these colours probe.

Fig. 4 presents the dependency of the variance in the colour gradient with the actual values of the $(g-i)$ and $(r-z)$ colour gradients. From this figure we learn that galaxies with redder cores (negative colour gradient) measured from the $(r-z)$ colour gradients, tend to have larger errors, due to the z band being the noisiest among the four in this study. The same is not true for the $(g-i)$ colour gradients. It can be seen in Fig. 4 that steeper gradients tend to have larger errors, for both colour gradients.

Fig. 3 shows that both the $(g-i)$ and $(r-z)$ colour gradients for sample *S20.5* have median values that are similar: -0.048 , -0.067 , respectively (-0.187 , -0.277 , when defining colour gradients as colour per decade in normalised radius). However, the longer negative tail of the distribution for the $(r-z)$ colour gradient is clear. This slight difference is likely to be due to the fact that redder stars contribute more in the $(r-z)$ than in the $(g-i)$ colour, giving rise to steeper gradients. However, the tilted distribution of the $(r-z)$ colour gradient variance shown in Fig. 4, would also be responsible, at least in part, for this difference.

We have also compared the distribution of colour gradients for the different luminosity-threshold selections defined in Table 1. There is not a clear change in the shape of the distributions for the different samples, just different numbers of galaxies. The change in median values from one sample to another is rather small: -0.050 , -0.049 , -0.044 for the median $(g-i)$ colour gradient of samples *S19*, *S20* and *S21*, respectively.

In appendix A we analyse some of the the systematic effects that could affect the distribution of colour gradients, including the ellipticity, the amount of light considered in the calculation and the effect of having close pairs of galaxies. Considering the result found in appendix A and the similar distributions for all the luminosity-threshold samples considered in this work, we can conclude that the results for the colour gradient distribution are robust.

Returning to Fig. 3, we can clearly see there that galaxies tend to have small internal colour variation, resulting in quite flat colour gradients. Nevertheless, the median of the distribution is negative, implying that, in general, galaxy centres are redder than their outer parts. As described in the introduction, Fig. 3 shows then that galaxies tend to have more metal rich cores that might also be hosting older stellar populations. Though, age gradients present larger dispersion than metallicity ones (MacArthur et al. 2009; Vlajić et al. 2009; Rawle et al. 2010; Tortora et al. 2010). This agrees with previous studies using smaller samples of galaxies (see e.g. Peletier et al. 1990; Michard 2005; Lee et al. 2008; Tortora et al. 2010).

A remarkable feature of Fig. 3 is that it presents a single peak. This result could be indicating that galaxies with different structural characteristics, late and early type galaxies, have undergone similar star formation histories. However, the distribution of colour gradients presented in Fig. 3 is much broader than a Gaussian. We have checked whether this is due to the observational errors using Monte Carlo simulations. We have found that taking into account the colour gradients variance, we still obtain a distribution narrower than the observed one. Thus, we demonstrate that the width and shape of the colour gradient distribution cannot be explained by the

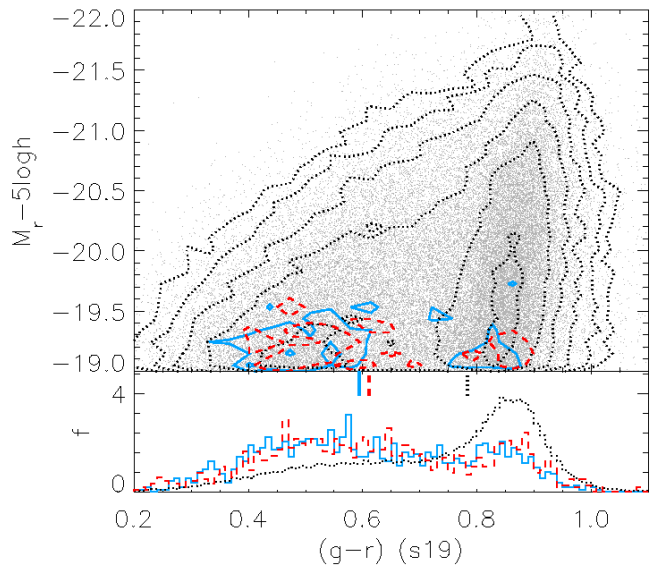


Figure 5. The upper panel shows the absolute magnitude in the r -band versus the global colour $(g-r)$ for galaxies within the sample *S19*. Contours increase by factors of two in density, illustrating the behaviour of galaxies within different ranges of $(g-i)$ colour gradient distribution. Dotted contours correspond to galaxies with $(g-i)$ colour gradients within the 2σ limits of the total distribution. Solid/Dashed contours present the distribution of those galaxies with their $(g-i)$ colour gradients above/below the 2σ limit of the distribution, i.e., with bluer/redder cores than the average trend. The lower panel shows the medians and the distributions of the $(g-i)$ colour gradients with the global $(g-r)$ colour for the three subsamples in the corresponding line types. Histograms are normalised to give unit area underneath.

error distribution alone and that galaxies do indeed present different intrinsic colour gradients. We find the colour gradient distribution to be best described as the superposition of the distributions of two populations of galaxies.

We will explore further this last aspect in §3.2 and §3.3. Before, we analyse the potentially different nature of those galaxies with extreme positive and negative colour gradients.

3.1 Positive and negative colour gradients

Here we study whether extremely steep colour gradients occur only in certain types of galaxies.

In Fig. 5 and Fig. 6 we explore the possibility for galaxies with positive and negative colour gradients to separate in a colour-magnitude or colour-concentration parameter space. In both plots, density contours correspond to the behaviour of three subsamples separated by their $(g-i)$ colour gradient values. We have set as boundaries the 2σ values corresponding to the $(g-i)$ colour gradient distributions of each sample. In this way we separate those galaxies with extreme colour gradients from the global trend.

Fig. 5 shows the absolute magnitude versus the global $(g-r)$ colour, while Fig. 6 presents $(u-r)$ versus light concentration. Both parameter spaces were explored by Blanton et al. (2003) and Driver et al. (2006), respectively. These studies showed the bimodality of galaxies, which separate in these spaces into early and late-type. In the Blanton et al. (2003) observations, the bimodality of SDSS galaxies is clear for galaxies fainter than $M_{0.1r} \sim -20$ (absolute magnitude at $z = 0.1$). A similar trend is found here for the

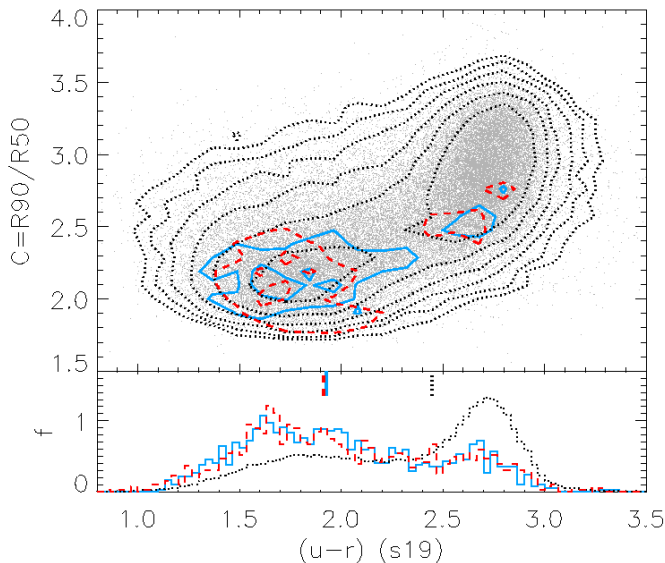


Figure 6. Similar to Fig. 5 but for $(u-r)$ vs concentration index.

faintest sample *S19*. The brighter samples, *S20*, *S20.5*, *S21*, do not show a clear bimodality due to the magnitude cut.

In Fig. 5 those galaxies with very steep colour gradients only appear at the faint end, corresponding to the region with the largest dispersion, but also with the largest errors in magnitude. Galaxies with very steep positive and negative colour are distributed similarly in Fig. 5.

Fig. 6 shows that galaxies with extreme colours neither separate in this parameter space. The same is seen when defining the colour gradient as colour per decade in normalised radius. Nevertheless, Fig. 6 shows a remarkable behaviour: the galaxies with the steepest colour gradients are not galaxies with high concentration indices. Galaxies with high concentration indices are generally passively evolving with minimal content of gas. Since few galaxies with high concentration index show steep colour gradients, then one expects that these steep colour gradients are more likely related to star formation. We will further explore this in §3.2.

From both Fig. 5 and Fig. 6 it is clear that galaxies with steep colour gradients, independently of their sign, appear in larger numbers towards the blue end of both the $(u-r)$ and $(g-r)$ global colour distributions.

Fig. 5 also shows that redder cores appear, on average, within redder galaxies than those with bluer cores. This difference is clearer for brighter samples, for which also the same tendency can be seen for the $(u-r)$ global colour.

We have also explored whether galaxies with very steep gradients appear separated when looking to parameter spaces that depend on age or metallicity against concentration index. In particular we have studied the variation with light concentration of the *D400* spectral index and the Lick index *Hb*, both of which are mostly sensitive to age. We have also compared concentration to the Lick indices *Mg2* and *Fe5335*, both closely related to the global metallicity of the galaxy.

We observe that both *Fe5335* and *Hb* stay quite flat with light concentration, which prevents the separation of galaxies in such parameter space. We find a similar bimodality in the parameter space *D4000* vs. *C*, to that reported by Kauffmann et al. (2003b) for the SDSS DR2. Moreover, we find that galaxies also separate into early and late-types in the parameter space *Mg2* vs. *C*. We find again

that galaxies with very steep gradients appear to have a wide range of indices values, basically covering the same range as the global trend. It is also interesting to note that this is independent of the steep colour gradients being positive or negative. The lack of a clear locus occupied by those galaxies with steep gradients in the different studied parameter spaces suggest that the existence of extreme colour gradients depend weakly on the global age or metallicity of galaxies.

The studied indices are measured within the SDSS DR7 fibre spectra, with a diameter of $3''$. We have studied the behaviour of a subsample of galaxies with $R50 \leq 1.7''$, i.e. galaxies with more than half of their light contained within the SDSS fibre spectra. This subsample exhibits similar tendencies to the global ones, except that in this case there are galaxies with steep colour gradients that have their light highly concentrated. A subsample of galaxies with only their cores measured within the SDSS spectra, with $R50 > 4.6''$, give a better match to the global trends, in the sense that the light concentration distributes in a similar way to the total sample. We also find similar trends for the *D4000* vs. *C*, when using the spectral index derived by the MPA/JHU collaboration. Therefore, the tendencies of the colour gradients with the SDSS age and metallicity indices can be considered as representative of the tendencies with the global ages and metallicities of galaxies without making any further consideration.

In summary, we find that extreme internal colour variations tend to happen within galaxies that are blue, with low concentration indices and in the faint end of the sample distribution. Though, these extreme variations can occur within galaxies with a wide range of ages and metallicities. Bluer cores preferentially appear in bluer galaxies. However, the difference between galaxies with extreme positive and negative colour gradients is small. This could be an indication that very negative and very positive colour gradients share a similar origin. If the internal colour variation was mainly due to supernova winds or localised star formation regions, then the spatial probability for these phenomena to happen should be quite flat within galaxies. In their work on early-type galaxies Rawle et al. (2010) suggested that for galaxies with a velocity dispersion below 140 km/s , metallicity gradients are tightly correlated with stellar mass, while above this threshold mergers are the main driver for setting the colour distribution within a galaxy. Thus, rather than a similar origin, we could be looking to different phenomena: AGN or gas poor mergers vs. gas rich mergers, occurring with a similar probability. It is clear then the difficulty on disentangling how very steep gradients were originated. Further work will be needed to understand the similar distributions of positive and negative colour gradients.

3.2 Colour gradients within early and late type galaxies

In this section we study the internal colour variation within early and late-type galaxies, using different parameters to classify galaxies into one of those categories.

The left panel in Fig. 7 shows for galaxies in the *S20.5* sample the variation of the $(g-i)$ colour gradient with the concentration index, *C*. As it can be seen in this plot, median colour gradients tend to be flatter for galaxies with higher values of the light concentration. In fact, the same is seen for all the studied colour gradients: $(g-i)$, $(g-r)$, $(r-z)$, $(r-i)$, $(i-z)$, in the different luminosity-threshold samples considered here. This was expected given the trends seen in the previous section. Due to the dispersion, this correlation is not statistically robust, with a Spearman coefficient of 0.19. However, the increase in the dispersion of observed colour

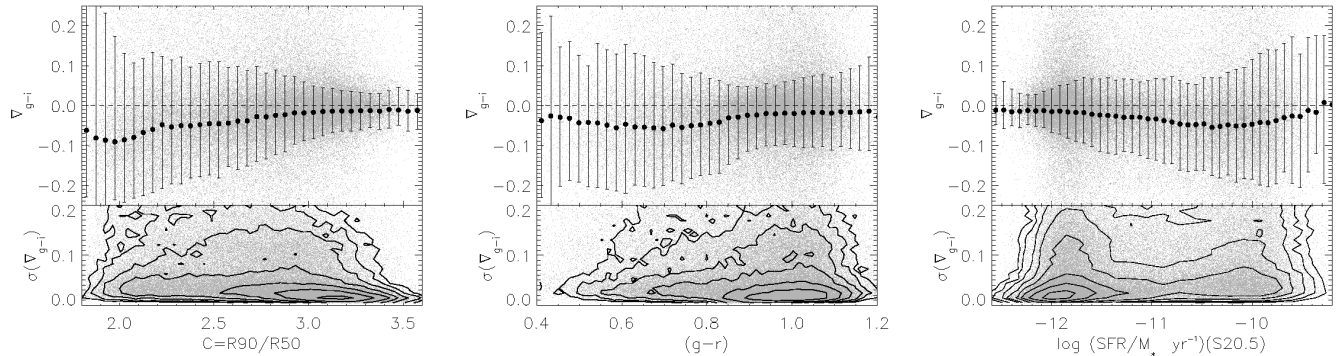


Figure 7. Variation with the concentration index (left), $(g-r)$ colour (middle) and specific star formation (right) of the $(g-i)$ colour gradient, top panels, and its error, bottom panels, for galaxies within the $S20.5$ sample. The panels showing colour gradients have superimposed median colour gradients values and their 1σ range. The panels showing the variance of the colour gradients present density contours with increments of a factor of two.

gradients is not correlated with a trend in the gradient errors and so, it is significant.

We find that early-type galaxies tend to have flatter colour gradients than late-type galaxies. Most spirals are classified as late-type and have an exponential light profile. In simple terms, these galaxies are formed by a bulge and a disk component. Bulges share features with early-type galaxies, being dominated by an old stellar population. Meanwhile, disks contain, in general, regions of star formation, providing an increase in the percentage of young stellar populations. These differences allow for greater colour variations to happen in comparison with early-type galaxies, whose characteristics are much more homogeneous.

Tortora et al. (2010) also found a similar trend for colour gradients with the Sérsic index, which is tightly related to the concentration index. These results also agree with the study by Weinmann et al. (2009), where they found that galaxies with $C < 3$ present steeper colour gradients.

Colour has also been widely used in the literature to split galaxies into early and late-types. The middle panel in Fig. 7 shows the variation of the $(g-i)$ colour gradient with the global $(g-r)$ colour of galaxies. In agreement with Fig. 5 and Fig. 6, it is clear in Fig. 7 that the redder a galaxy is the flatter the colour gradient is expected to be. The trend is similar to that seen for the concentration index: early-type galaxies present flatter colour gradients. However, the correlation with global colours is weaker than with the concentration index, with Spearman index of ~ 0.10 . This could indicate that colour gradients depend more strongly on morphological characteristics than on global colours. For example if the colour gradient is set by the relative contribution of bulge and disc for late-type galaxies, one would expect that it would correlate more strongly with concentration index than with global colour.

For a given mass range, late-type galaxies are, in general, forming stars more efficiently than early-types ones. The right panel in Fig. 7 presents the variation of colour gradient with the specific star formation derived by the MPA/JHU collaboration. With a Spearman index of ~ 0.14 , the correlation between these two parameters is not statistically robust, likely due to the increase of the dispersion for those galaxies with higher specific star formation rates. The variance of the colour gradients does not determine the dispersion increase, which makes, again, the tendency significant.

Assuming a constant star formation, the inverse of the specific star formation, M_*/SFR , will provide an estimation of the time it took a galaxy to build up its observed stellar mass. Thus, higher values of specific star formation will correspond to younger galax-

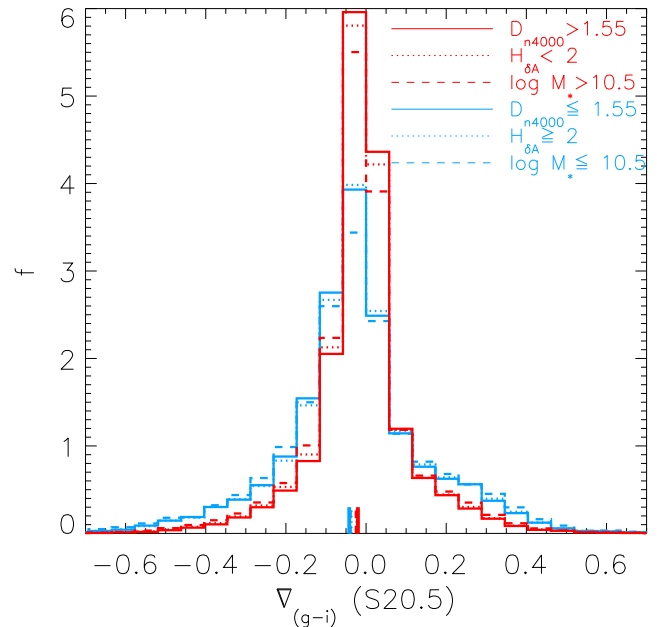


Figure 8. Distribution of the $(g-i)$ colour gradients within galaxies from $S20.5$ sample split into early (red lines) and late (blue lines) types using different parameters: 4000 Å break, solid lines, $H_{\delta A}$ Balmer index, dotted lines, stellar mass, dashed lines. Median values are shown as short, thick lines of the corresponding type. Histograms are normalised to give unit area underneath.

ies, or at least, with a larger percentage of young stars. The found correlation between the specific star formation and the colour gradient indicates that steeper gradients appear for galaxies with higher percentages of young stars.

From Fig. 7 we can conclude that early-type galaxies have smaller internal colour variations compared to late-type galaxies.

We have also compared the shape of the distribution of colour gradients within early and late-type galaxies, selected accordingly to either concentration index, global colour or specific star formation, finding that early-type colour gradients have narrower distributions than late-types. As can be seen in Fig. 8 this is also true when separating galaxies into early and late-types using other parameters.

Fig. 8 shows the $(g-i)$ colour gradient distribution for galaxies from the $S20.5$ sample separated into early and late-types following the Kauffmann et al. (2003b) work, by using the following

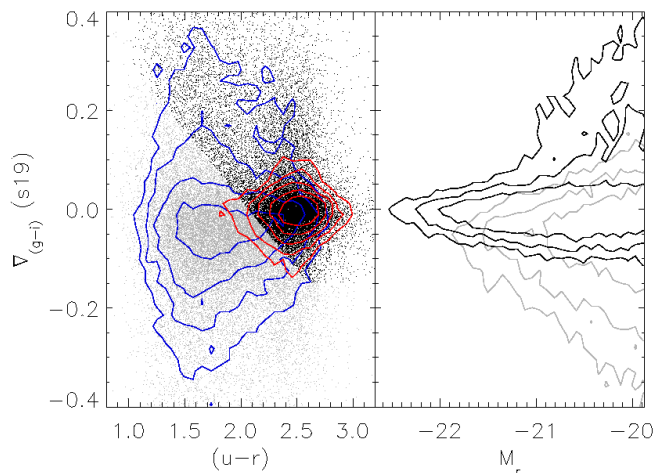


Figure 9. Both panels show data from galaxies with $b/a \leq 0.6$, within the *S19* sample. Galaxies have been separated into early, in black, and late-type galaxies, in grey, following Park & Choi (2005) criterion. Contours represent a factor of two change in density. *Left:* $(u-r)$ colour vs. $(g-i)$ colour gradient. Blue contours show the density for galaxies with $C \leq 2.6$, those in red correspond to galaxies with $C > 3$. *Right:* Absolute magnitude in r band vs. $(g-r)$ colour gradients.

parameters derived by the MPA/JHU collaboration: the D_n4000 index, sampling the spectral 4000\AA break, the Balmer index $H_{\delta A}$ and the logarithmic stellar mass. Mass does not clearly separate galaxies into early and late-types, but the characteristics of galaxies with masses below or above $10^{10.5} M_{\odot}$ are rather different (Kauffmann et al. 2003b). Despite median values being quite close for early and late-types galaxies, it is apparent that late-type galaxies present a wider distribution with more extended tails than for the case of the early-type galaxies distribution.

As found here, Tortora et al. (2010) also reported a larger dispersion for colour gradients among late-type galaxies. Suh et al. (2010) found that although most of the early-type galaxies have quite flat colour gradients, there is $\sim 30\%$ with residual star formation that produces steeper colour gradients, in consonance with the distributions reported here.

In summary, the probability for finding strong internal colour variations within early-type galaxies is lower than for late-type galaxies.

3.2.1 Early and late type galaxies based on their colour gradients

Choi et al. (2007) have studied the behaviour of colour gradients with absolute magnitude for early and late-type galaxies, separated by their position in the colour gradient versus colour parameter space as defined by Park & Choi (2005). In order to compare our results with the Choi et al. (2007) study we have also separated galaxies into early and late-type according to the Park & Choi (2005) method. Our definition of colour gradients is different since they just compare the light outside and inside half the Petrosian radius of galaxies. Moreover, they use magnitudes K-corrected to redshift 0.1. We have not applied any corrections to take into account these differences, we will thus compare tendencies qualitatively, rather than actual values.

The left panel in Fig. 9 shows the $(u-r)$ colour versus the $(g-i)$ colour gradient, using black/grey dots for those early/late-type galaxies according to Park & Choi (2005) criterion. In the

same panel we have superimposed density contours for galaxies with different light concentrations: $C \leq 2.6$ and $C > 3$. We can see there that the Park & Choi (2005) classification scheme agrees quite well with separations based on the concentration index.

The right panel in Fig. 9 shows the $(g-i)$ colour gradients as a function of absolute magnitude. Fig. 9 shows that those galaxies classified as early-types have a very constant median colour gradient with absolute magnitude. The same behaviour is reported by Choi et al. (2007) La Barbera et al. (2005). Early-type galaxies within the *S19* sample, especially those fainter than $M_r \sim -21$, present values with increasing dispersion towards positive values, i.e. towards having bluer cores. In this case this could be related to the branch of early-type galaxies with residual star formation, as the E+A galaxies⁶ reported by Park & Choi (2005). Indeed, in their work they showed that one of the advantages of their way of separating galaxies is that E+A galaxies are classified as early-types, although they are bluer and less concentrated than most early-type galaxies. In fact the only difference found when using the concentration index to separate galaxies into early and late-types is that this increase in dispersion towards bluer cores within early-types disappears.

Unlike global galactic colours, the internal colour variation do not relate clearly to the luminosity of galaxies, though median colour gradients tend to be steeper at brighter magnitude bins. For fainter magnitudes than the ones studied here, Choi et al. (2007) observed that the colour gradients of late-type galaxies increase with magnitude. Nevertheless, within the magnitude range studied here the median colour gradients reported by Choi et al. (2007) also stay quite flat with magnitude. Bakos et al. (2008) studied the internal colour variation within 85 spiral galaxies finding that it is almost constant for a given luminosity.

In comparison to early-types, late-type galaxies have steeper colour gradients and present a larger dispersion that increases for fainter magnitudes. These results are in agreement with Choi et al. (2007) and in consonance with our previous findings.

3.2.2 Velocity dispersion and stellar mass

Due to the complexity for obtaining the velocity dispersion, the SDSS provides measurements only for galaxies with a clean spectrum typical of an early-type at $z < 0.4$. The subsample of galaxies with a reliable measurement of velocity dispersion presents slightly flatter colour gradients with larger velocity dispersions. Such tendency is not statistically robust for the $(g-i)$ colour gradient, with an Spearman index of ~ 0.12 , due to the increase in dispersion. Though, as for the parameters studied before, the distribution of errors alone cannot explain the change in dispersion, which makes the tendency significant.

Stellar mass and velocity dispersion are tightly correlated. The trend seen for the velocity dispersion is supported by the correlation that we find between the $(g-i)$ colour gradient and the stellar mass derived by the MPA/JHU collaboration. For a similar range in both masses and luminosity, our result for the most massive galaxies to present flatter colour gradients agrees with previous studies (Weinmann et al. 2009; Suh et al. 2010; Tortora et al. 2010).

Fig. 10 shows the variation with stellar mass of the median

⁶ E+A galaxies are dominated by an old stellar population but their spectra show signatures of the occurrence of minor star formation bursts. See Yamauchi & Goto (2005) for a study of colour gradients in E+A galaxies.

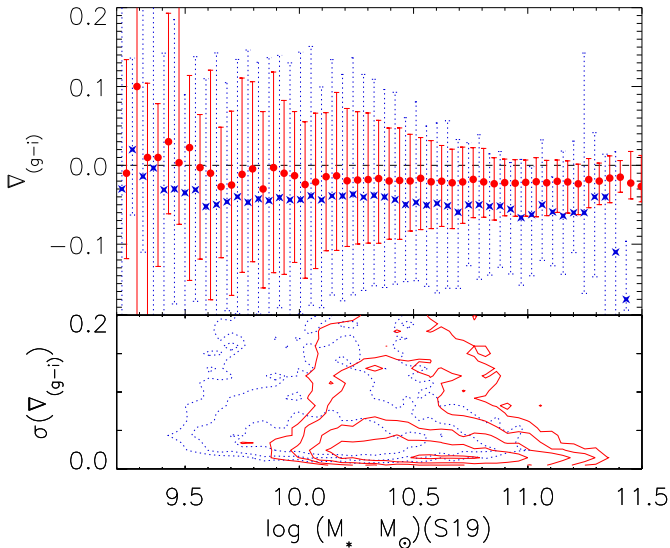


Figure 10. Variation with stellar mass of the median $(g-i)$ colour gradient for early, circles, and late-type galaxies, stars, within sample *S19*. Error bars corresponds to the 1σ range in dispersion. Bottom panel shows the variance of colour gradients within early, solid contours, and late-type galaxies, dotted contours. Contour plots increases by a factor of two in density.

$(g-i)$ colour gradient for early, with $C > 2.6$, and late-type galaxies, with $C \leq 2.6$. The median of the colour gradient distributions for both type of galaxies remain quite flat for masses above $M \geq 10^{9.5} M_\odot$. Less massive galaxies tend to present flatter or even positive colour gradients, although the dispersion is much larger.

Our sample of galaxies contain rather massive galaxies, with $M \geq 10^9 M_\odot$. For this range of masses there is a wide dispersion for the star formation rates (Brinchmann et al. 2004), thus it is difficult to connect this result with the different mechanisms that are able to produce colour gradients. Splitting our sample into early and late types we find that only those early-type galaxies with $M_* < 10^{9.5} M_\odot$ within the *S19* sample present a median positive colour gradient. Spolaor et al. (2009) have studied the dependency of metallicity gradients with stellar mass finding them to be tightly related if $M_* \leq 3.5 \times 10^{10} M_\odot$, as predicted by pure monolithic collapse models (e.g. Chiosi & Carraro 2002), while more massive galaxies do not appear to show this relation, as other studies previously proved (Michard 2005; Sánchez-Blázquez et al. 2006; Tortora et al. 2010). For those galaxies in the lowest stellar mass range, the metallicity gradient becomes shallower with decreasing mass, which could translate into age gradients having a dominant effect on the colour gradients. This will provide the possibility to invert the colour gradients. In general, those early-type galaxies at $z = 0$ with the lowest mass could present higher star formation rates than more massive ones (De Lucia et al. 2006), which in turn could provide the existence of steeper positive colour gradients (bluer cores). We find a similar result for late-type galaxies, in the sense that only those galaxies in the lowest stellar mass bins present null or positive median colour gradients values.

The tendency found for early-type galaxies in Fig. 10 agrees with the studies from Suh et al. (2010); Tortora et al. (2010), and supports the previous idea for the existence of bluer cored early-type galaxies only in the lowest mass bins.

In the case of late-type galaxies, localised regions of star formation can also affect the colour gradients but dust and stellar migration can also have a significant impact on them

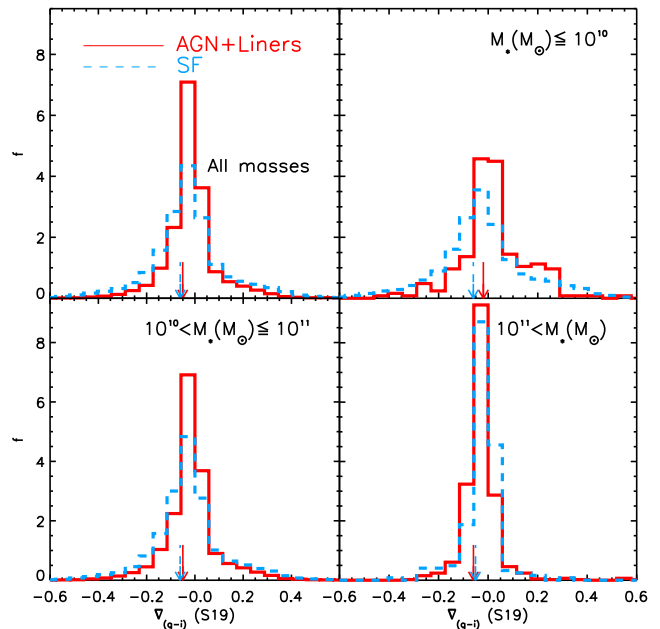


Figure 11. Distribution of the $(g-i)$ colour gradients within galaxies from the *S19* sample, separated into AGN plus LINERS (solid line) and star forming galaxies (dashed line) following Brinchmann et al. (2004). The top panel shows the distribution for all the galaxies in the sample, while the rest show the distribution within the mass range specified in the legend. Arrows show median values. Histograms are normalised to give unit area underneath.

(Sánchez-Blázquez et al. 2009; Vlajić et al. 2009). Stellar migration happens immediately after the formation of the wave density that leads to the formation of spiral arms, but also after the formation of bars or disk instabilities that can be triggered by tidal forces. Stellar migration is strongest for the most massive galaxies and tends to wipe out initial metallicity gradients, and, therefore, colour ones. This effect rises age gradients opposed to the metallicity ones, though the dispersion for these increase with mass (Rawle et al. 2010). The combined effect of age and metallicity gradients for massive galaxies can explain why we find the colour gradient to stay quite flat for late-type galaxies of different masses. Tortora et al. (2010) found a clear steepening with mass for the colour gradient within late-type galaxies. As mention before, we find that the least massive galaxies in our sample present flatter median colour gradients, i.e., we find a very slight trend in the same direction as the one reported by Tortora et al. (2010). However, the slopes of these trends are different. The origin of this difference is unclear but it could be related with the different definitions of colour gradient or the sample selection.

3.3 Colour gradients, star formation and nuclear activity

Beside stellar winds and migrations, the nuclear activity could also be responsible for the existence of anomalous internal colour variations within galaxies. Menanteau et al. (2005) found one blue nucleated spheroid with star formation associated with the presence of an AGN. If the association was found to be general, this will be a stronger indicative for a delayed galactic formation.

Here we try to disentangle the effects of star formation and nuclear activity as responsible for setting colour gradients. We use the classification done by the MPA/JHU collaboration for the SDSS DR7 based on the one from Brinchmann et al. (2004),

which makes use of the location of a galaxy in the parameter space $\log([OIII]5007/H\beta)$ versus $\log([NII]6585/H\alpha)$, the so called BPT diagram (Baldwin et al. 1981), taking into account the signal to noise S/N of the spectral lines. In this parameter space it is possible to separate star forming galaxies from those with nuclear activity, though there is a region where galaxies are considered as composites. Due to the requirement of a minimum S/N value for the lines, not all galaxies can be classified following this scheme.

We have explored the locus occupied in the BTP diagram by those galaxies with very steep colour gradients, finding that they distribute following the mean trend.

Fig. 11 presents the distribution of the $(g-i)$ colour gradients within galaxies from the *S19* sample, separated into galaxies with nuclear activity and star forming galaxies. The left upper panel of this figure presents the whole sample, showing that steep colour gradients are more likely to appear within star forming galaxies rather than those with nuclear activity. In fact, there is a minute increase, $\sim 2\%$, in the percentage of galaxies classified as star forming among those with steep colour gradients, compared with the mean trend. This last tendency goes in the direction expected from the above discussions.

The studied early-type galaxies present a higher percentage of galaxies with nuclear activity, independently of their colour gradients. Thus Fig. 11 could be driven by the different distribution of colour gradients for early and late-type galaxies seen in §3.2.

The remaining panels explore the colour gradient distributions for galaxies within three mass ranges. Kauffmann et al. (2003c) found that different levels of nuclear activity appears in galaxies with different masses. Galaxies with masses below $10^{10}M_{\odot}$ could present a weak AGN, but not a strong one. In this mass range we observe that those galaxies from the *S19* sample that are hosting an AGNs present a higher percentage of bluer cores than those forming stars. The other studied samples of galaxies do not present this difference, but yet, they contain fewer low mass galaxies. The AGN within these low mass galaxies could be driving dust out of the central galactic region, lowering its internal extinction, which could provide bluer cores.

Galaxies more massive than $10^{10}M_{\odot}$, host most of the AGN activity. As expected from §3.2.2, the colour gradient distribution for the most massive galaxies is quite narrow, with few galaxies presenting steep colour gradients. The median colour gradients for massive galaxies remain quite constant and comparable to the global median.

Our results suggest that nuclear activity is a marginal driver for creating steep colour gradients, and that it is overcome by the dependency between colour gradients and morphological type, at least for those galaxies with masses above $10^{10}M_{\odot}$.

3.4 Colour gradient change with redshift

Comparing the two panels in both Fig. 5 and Fig. 6 for the samples under study, we have observed that galaxies with steep colour gradients tend to be redder when moving to samples including galaxies at higher redshifts. The global sample also gets redder when going from sample *S19* to *S20.5*, but the variation is smaller. We have observed that colour gradients do not depend strongly on absolute magnitude, except for an increase in the scatter at the faintest end. Thus, this result could suggest a stronger evolution for those galaxies with steeper colour gradients in the recent past.

Fig. 12 shows the variation of the $(g-i)$ colour gradient with redshift for early and late-type galaxies within the *S20.5* sample. For both types of galaxies the median colour gradients stay constant

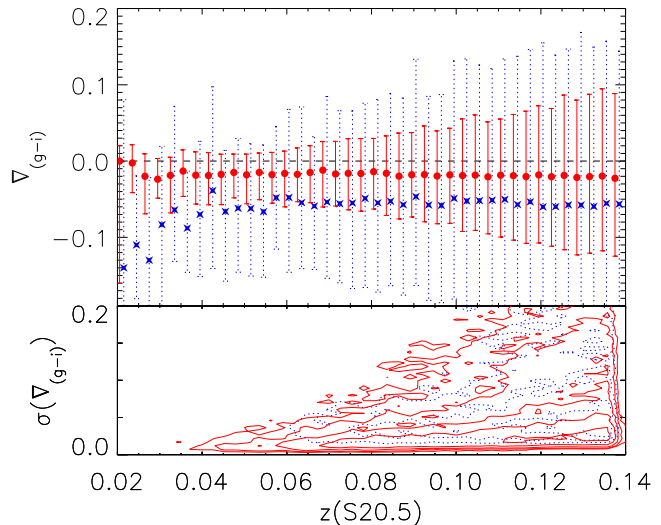


Figure 12. Similar to Fig. 10 for the variation with redshift of the $(g-i)$ colour gradients within galaxies in samples *S20.5*.

with the redshift, while the dispersion and errors increase. We find that for a fixed magnitude the dispersion in the colour gradient as a function of redshift is highly reduced. The opposite is not true. This is in agreement with Bakos et al. (2008).

We observe that it is more probable to find a galaxy with a steeper colour gradient at higher redshift. However, this trend of the dispersion could be driven by the errors distribution.

We have explored visually 48 early-type galaxies randomly selected among those with positive gradients, outside the 1σ range, and within the median value to explore the possibility of those early-type galaxies with steeper colour gradients to be more affected by artifacts. We find the same amount of galaxies either close to stars or other galaxies among both groups of galaxies. Thus, the observed tendency does not appear to be due to a higher presence of artifacts among those early-types with steeper colour gradients.

The fact that median colour gradients do not appear to evolve at $z < 0.17$, points out that most the star formation activity occurred previously.

4 SUMMARY AND CONCLUSIONS

In this paper we have studied the internal colour variation within galaxies from the SDSS DR7, with both clean photometry and spectroscopic measurements. We have obtained the global (K+e)-correction by using SED templates from PEGASE and applied them to each galaxy in order to divide our initial sample into luminosity-threshold ones, with redshifts up to $z = 0.17$. These samples are the largest used for studying the internal colour variation.

The internal colour variation has been quantified through the slope of the relation between radial colour and the galactic radius normalised to the one containing half the total galactic light, $R50$. Colour gradients have been obtained from the SDSS measurements of surface brightness circularly averaged in concentric annuli. Observational errors have been taken into account using a Monte Carlo method in the colour gradient calculation. This approach is independent of previous ones in the literature, therefore the agreement with earlier works underscores the robustness of the colour gradient as a useful parameter for studying particular aspects of galactic evolution.

In agreement with previous studies, we have found that colour gradients distribute around median values that are negative but close to zero, i.e. galaxies, independently of their morphological type, tend to have slightly redder cores than their external parts.

We have explored some of the possible systematics that could affect the measurement of the colour gradients. In particular we have explored the possible dilution due to the fact that we start our calculation of the colour gradient from a circularly averaged surface brightness profile. We observe that very elongated galaxies tend to have steep colour gradients, the opposite trend to the one expected if they were diluted. According to Choi et al. (2007), steep colour gradients within elongated galaxies are due to their internal dimming. In the calculation of the colour gradients we have left out the innermost annuli, since they are the ones most affected by seeing. We have explored the effect of obtaining colour gradients using different number of annuli, finding that for the range in which we work our results on colour gradients are robust. We find that galaxies with larger half light radii tend to have steeper colour gradients, being an intrinsic characteristic of galaxies and not an artifact.

We have selected a subsample of close pairs of galaxies that appear to be interacting. The sample is small, far less than 1% of the total sample, and it represents an inferior limit of such close pairs of galaxies with respect to what the total percentage that might be found when considering the whole photometric SDSS sample. Despite the small number of galaxies in this sample, we find a larger proportion of galaxies with bluer cores here than in the whole population sample. As close pairs are more likely to be interacting and normally these interactions are associated with an enhancement of star formation, this supports the connection between steep colour gradients and recent bursts of star formation.

We find that the colour gradient distribution does not follow a Gaussian due to an excess of galaxies in the tails that cannot be explained alone by the errors distribution. A double-Gaussian fits better the colour distribution, pointing out a possible contribution of two distinctively different galaxy classes. Separating the initial sample of galaxies into early and late-types we find that the distribution for colour gradients within late-type galaxies is more extended than that for early-types. Nevertheless, the distribution of early-type galaxies is still broader than a Gaussian. We find this excess of steep colour gradients to be likely related to age gradients, AGN activity or an unusual dust content.

The observed distribution of colour gradients can be understood as a consequence of entangled effects. Gradients produced in mergers depend on the time scales that interplay in their creation and the mixing of elements that can contribute to their destruction. Galaxies observed at different epochs after a gravitational interaction can present colour gradients evolving with time. Nevertheless, even when observing galaxies at a similar time after a merger one expects to find a distribution of colour gradients and not a single value, since the metallicity enrichment appear to be highly non-uniform, due to the multi-phase nature of the intergalactic medium (Springel & Hernquist 2003). Besides, Kobayashi (2004) simulated the formation of early-type galaxies through different kind of mergers, finding that the metallicity gradients (the main origin of colour gradients) strongly depend on the ratio of stellar masses and gas content between the progenitors. Moreover, even if early-type galaxies were formed in a "monolithic collapse", for a given stellar mass there would be certain scatter in star formation efficiencies which provides a scatter in colour gradients (e.g. Pipino et al. 2010). For late-type galaxies the dust content and the bulge to disk relation depending on the observing inclination angle, together with the complicated patterns of stars migrations that fol-

low the spiral arm formation, can also enhance the colour gradient dispersion, at least temporally (Sánchez-Blázquez et al. 2009).

Galaxies with steep gradients share some global properties independently of presenting bluer or redder cores. Nevertheless, redder cores happen, on average, within galaxies redder than those with bluer cores. We have also observed that galaxies with high concentration values do not present steep colour gradients. It is known that mergers increase the galactic size and that galaxies with highly concentrated light have features indicating either a passive evolution in their recent past or the lack of gas, ruling out the possible existence of great internal colour variations. Thus, both results suggest the existence of a relation between colour gradients and the recent formation history of galaxies, in the sense that very steep colour gradients are likely related to recent star bursts.

We have found that galaxies with steeper colour gradients are more likely to be late-types according to either their structural parameters or to their specific star formation, i.e., a higher presence of young stars. It is interesting to note that we have found that colour gradients are less tightly related to global colours than the concentration index. Park & Choi (2005) found out that the parameter space colour-colour gradient could be very useful to select galaxies matching their optical morphology at low redshifts. Our study indirectly supports theirs, suggesting that colour gradients origins are more related to the recent formation history of galaxies, the kind of gravitational interactions recently suffered, than with the global galactic colours. Different studies (see e.g. Schawinski & Lintott et al. 2009) are finding spheroidal galaxies with blue colours and red spirals. This proves the usefulness of a parameter like the colour gradient that is sampling something that cannot be seized through the global colour.

We have found that the possible correlation between colour gradients and nuclear activity is overcome by the stronger relation with galactic type, since nuclear activity appears more common among early-types in our sample of galaxies.

At intermediate redshift, $0.37 < z < 0.83$, Menanteau et al. (2001) found that 30% of field spheroids (classified based on their morphological parameters) show an unusual internal colour variation. Menanteau et al. (2001) associated this large colour variation with either star formation or AGN activity, in consonance with our results for a closer sample of galaxies.

Within the redshift range studied here, the colour gradients within early-type remain rather constant, implying that these galaxies had their last residual bursts of star formation at earlier times.

The results presented in this work agree with previous studies, though, here we are more dominated by the scatter due to the larger sample explored. Nevertheless, our results are very robust since they hold for the four studied luminosity-threshold samples.

Colour gradients are normally defined in the literature as the colour variation as a function of the logarithm of the radius. Here we have used the variation of colour as a function of the radius itself. Using the former definition we have checked that we obtain qualitatively similar trends for colour gradients, except that their distribution covers a broader dynamical range. For the *S20.5* sample, the median values of these distributions are -0.187 and -0.277 , respectively for the $(r - z)$ and $(g - i)$ colour gradients. In our calculation of colour gradients we assume the observational errors in both colours and radii to be normally distributed. When using the logarithm of normalised radius, the error distribution deviates from a Gaussian. Thus, in order to make an accurate comparison we should modify the way we are including the observational errors in our calculation. This is likely to have a fundamental effect on the estimated errors, while colour gradients would remain practically

unchanged. Leaving apart this issue, when defining the colour gradient as colour variation as a function of the logarithm of the radius we find qualitatively similar tendencies to the ones previously reported. The correlations appear stronger when defining colour gradients in this way, due to the enhanced dynamical range.

The fact that steep colour gradients are linked with a higher presence of young stars could provide an alternative method for exploring the interactions between galaxies. A thorough spectral analysis of those galaxies which present extreme colour variations could help us to better understand the mechanisms that generate either bluer or redder cores within galaxies.

ACKNOWLEDGEMENTS

We thank J. Lucey, I. Ribas and R. Smith for their helpful comments. Thanks to C. Baugh for reading the manuscript. VGP is supported by a Science and Technology Facilities Council rolling grant and acknowledges past support from the Spanish Ministerio de Ciencia y Tecnología.

REFERENCES

- Abazajian K. et al., 2009, *ApJS*, 182, 543
 Bakos J., Trujillo I., Pohlen M., 2008, *ApJL*, 683, L103
 Baldwin J. A., Phillips M. M., Terlevich R., 1981, *PASP*, 93, 5
 Barbera L., F. Carvalho d., R R., 2009, *ArXiv e-prints*
 Begelman M., de Kool M. and Sikora M., 1991, *ApJ*, 382, 416B
 Blanton M. R. et al., 2003, *APJ*, 594, 186
 Brinchmann J., Charlot S., White S. D. M., Tremonti C., Kauffmann G., Heckman T., Brinkmann J., 2004, *MNRAS*, 351, 1151
 Bruzual A. G. and Charlot S., 1993, *ApJ*, 405, 538
 Charlot S., Worthey G. & Bressan A., 1996, *ApJ*, 457, 625
 Chiosi C., Carraro G., 2002, *MNRAS*, 335, 335
 Choi Y.-Y., Park C., Vogeley M. S., 2007, *ApJ*, 658, 884
 Cooper A. P. et al., 2009, *ArXiv e-prints*
 de Boor C., 1978, *A practical guide to splines*. Applied Mathematical Sciences, New York: Springer, 1978
 De Lucia G., Springel V., White S. D. M., Croton D., Kauffmann G., 2006, *MNRAS*, 366, 499
 Driver S. P., et al. 2006, *MNRAS*, 368, 414
 Ferreras I., Lisker T., Pasquali A., Kaviraj S., 2009, *MNRAS*, 395, 554
 Fioc M., Rocca-Volmerange B., 1997, *A&A*, 326, 950
 Fukugita M., Shimasaku K., Ichikawa T., 1995, *PASP*, 107, 945
 Hamilton D., 1985, *ApJ*, 297, 371
 Hinkley S., Im M., 2001, *ApJL*, 560, L41
 Kauffmann G. et al., 2003a, *MNRAS*, 341, 33
 Kauffmann G. et al., 2003b, *MNRAS*, 341, 54
 Kauffmann G. et al., 2003c, *MNRAS*, 346, 1055
 Kobayashi C., 2004, *MNRAS*, 347, 740
 La Barbera F., de Carvalho R. R., Gal R. R., Busarello G., Merluzzi P., Capaccioli M., Djorgovski S. G., 2005, *ApJL*, 626, 19
 Larson R. B., 1974, *MNRAS*, 169, 229
 Lee J. H., Lee M. G., Park C., Choi Y.-Y., 2008, *MNRAS*, 389, 1791
 Li, Z. and Han, Z., 2007, *A&A*, 471, 795
 MacArthur L. A., González J. J., Courteau S., 2009, *MNRAS*, 395, 28
 Menanteau F., Abraham R. G., Ellis R. S., 2001, *MNRAS*, 322, 1
 Menanteau F., et al. 2005, *APJ*, 620, 697
 Michard R., 2005, *A&A*, 441, 451
 Oke, J. B. and Sandage, A., 1968, *ApJ*, 154, 210
 Park C., Choi Y.-Y., 2005, *ApJL*, 635, L29
 Peletier R. F., Davies R. L., Illingworth G. D., Davis L. E., Cawson M., 1990, *AJ*, 100, 1091
 Pipino A., D’Ercole A., Chiappini C., Matteucci F., 2010, *ArXiv e-prints*
 Poggianti B. M., 1997, *A&ASS*, 122, 399
 Rana N. C., Basu S., 1992, *A&A*, 265, 499
 Rawle T. D., Smith R. J., Lucey J. R., 2010, *MNRAS*, 401, 852
 Roche N., Bernardi M., Hyde J., 2009, *MNRAS*, 398, 1549
 Sánchez-Blázquez P., Courty S., Gibson B. K., Brook C. B., 2009, *MNRAS*, 398, 591
 Sánchez-Blázquez P., Gorgas J., Cardiel N., 2006, *A&A*, 457, 823
 Schawinski K., Lintott et al. 2009, *MNRAS*, 396, 818
 Scodreggio, M. 2001, *AJ*, 121, 2413
 Shimasaku K., 2001, *AJ*, 122, 1238
 Spergel D. N. et al., 2003, *ApJS*, 148, 175S
 Spolaor M., Proctor R. N., Forbes D. A., Couch W. J., 2009, *ApJL*, 691, L138
 Springel V., Hernquist L., 2003, *MNRAS*, 339, 289
 Strateva I., 2001, *AJ*, 122, 1861
 Strauss M. A., et al. 2002, *AJ*, 124, 1810
 Stringer M. J., Benson A. J., 2007, *MNRAS*, 382, 641
 Suh H., Jeong H., Oh K., Yi S. K., Ferreras I., Schawinski K., 2010, *ApJS*, 187, 374
 Tamura N., Ohta K., 2003, *AJ*, 126, 596
 Tamura N., Ohta K., 2004, *MNRAS*, 355, 617
 Tortora C., Napolitano N. R., Cardone V. F., Capaccioli M., Jetzer P., Molinaro R., 2010, *ArXiv e-prints*
 Vlajić M., Bland-Hawthorn J., Freeman K. C., 2009, *ApJ*, 697, 361
 Weinmann S. M., Kauffmann G., van den Bosch F. C., Pasquali A., McIntosh D. H., Mo H., Yang X., Guo Y., 2009, *MNRAS*, 394, 1213
 Worthey G., 1994, *ApJS*, 95, 107
 Wu H., Shao Z., Mo H. J., Xia X., Deng Z., 2005, *ApJ*, 622, 244
 Yamauchi C., Goto T., 2005, *MNRAS*, 359, 1557
 York D. G., Anderson Jr. J. E., Anderson S. F., SDSS collaboration 2000, *AJ*, 120, 1579

APPENDIX A: POSSIBLE SYSTEMATIC EFFECTS IN THE COLOUR GRADIENTS

A1 Effect of the ellipticity on the colour gradient

We obtain colour gradients from surface brightness measurements that are circularly averaged. Thus, colour gradients within elongated galaxies could be diluted. To address this issue we have separated galaxies within sample *S20.5*, the most populated one, into different ranges according to the ratio between the projected minor and major axes of the galaxies in the *r*-band, b/a . The top panel of Fig. A1 shows the variation of the $(g - i)$ colour gradient with b/a . We can see that more elongated galaxies present steeper colour gradients, with median values varying from -0.07 for galaxies with $b/a < 0.4$ to -0.04 for $b/a > 0.8$. This tendency appears independently of the band used to define b/a , except for the $(r - z)$ colour gradients, where all median values are similar, ~ -0.07 , independently of their b/a value. The same tendency of steeper gradient for more elongated galaxies is found for galaxies in the other studied samples. It is also seen when colour gradients are defined as the variation of colour per logarithmic normalised radius.

The bottom panel of Fig. A1 shows that the distribution of the

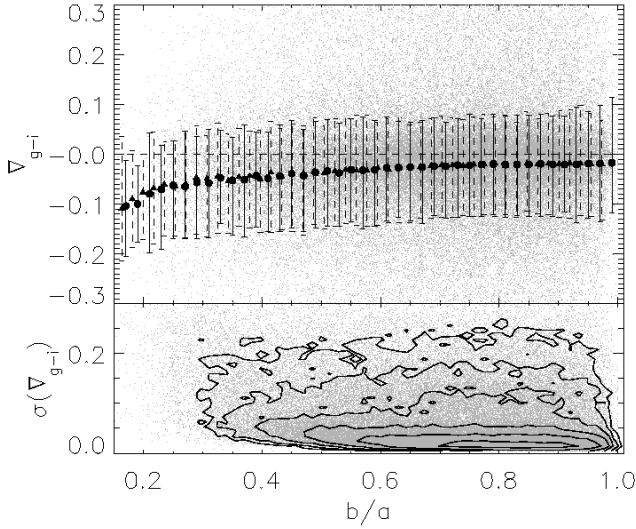


Figure A1. Variation of $(g-i)$ colour gradients with b/a in the r-band, top panel, and its errors, bottom panel, for galaxies within the *S20.5* sample. In the top panel we have superimposed median colour gradients values and their 1σ range for b/a in the r-band, circles with solid error bars, but also for b/a in the g-band, triangles with dashed error bars. The bottom panel shows density contours with increments of a factor of two.

error does not appreciably change as a function the projected axis ratio. Thus, the error distribution is not enough to explain the slope change of the median values around $b/a < 0.3$ seen in the top panel of Fig. A1.

This result shows that the dilution of colour gradients due to the use of circularly averaged surface brightness does not erase colour gradients although it may still dilute them somewhat.

Galaxies in the range $b/a < 0.4$ are late-types. Very inclined late-type galaxies are most affected by their internal absorption, something that could explain their steeper colour gradients. Due to their small gas content, early-type galaxies properties are not expected to be affected by their inclination.

Choi et al. (2007) studied the dimming effect for inclined late-type galaxies finding that it is better to exclude those with $b/a < 0.6$ when studying properties that could be affected by galactic internal dimming. Considering only galaxies with $b/a > 0.6$, we find that the linear variation of the median of the $(g-i)$ colour gradient with b/a has a slope smaller than 0.02, for all of the luminosity-threshold samples considered in our study. As expected from the large dispersion found in Fig. A1, the Spearman coefficient is too small to support statistically such a linear relation. Therefore, we can conclude that colour gradients do not vary in a significant manner with b/a , except for very inclined late-type galaxies, which are most likely affected by their internal dimming. Since the z-band is the least affected by dust extinction, this last result is consistent with the lack of $(r-z)$ colour gradient variation with b/a .

A2 Effect of the number of annuli considered for the colour gradient

Here we study the bias that we could be introducing by leaving out the innermost light, $R < 0.67''$, of the galaxy. In section §2 it was pointed out that the *S21* sample contains galaxies with half

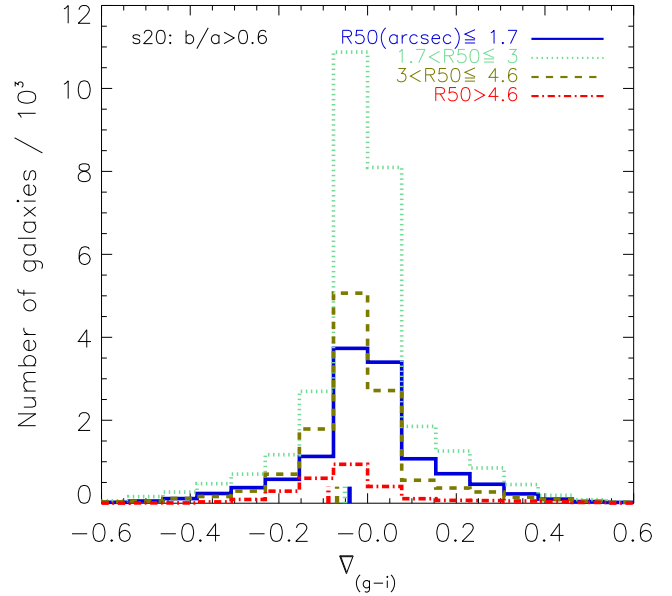


Figure A2. Distribution of $(g-i)$ colour gradients for galaxies with $b/a > 0.6$, within the *S20* sample separated by the radius containing half their light: $R50 \leq 1.7''$ (outer radius of 4th annulus, solid line), $1.7'' < R50 \leq 3''$ (limits of the 5th annulus, dotted line), $3'' < R50 \leq 4.6''$ (limits of the 6th annulus, dashed line), $R50 > 4.6''$ (outside the 6th annulus, dot-dashed line).

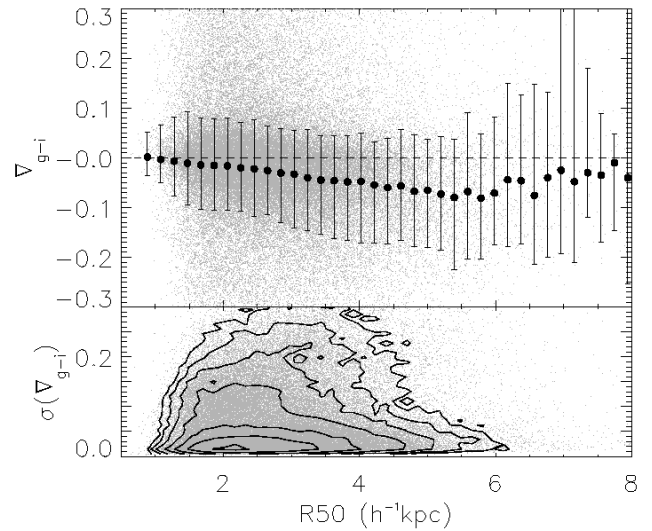


Figure A3. Similar to Fig. A1 for the radius containing half the total light ($h^{-1}kpc$) within galaxies from the *S20* sample.

light radii, $R50$, within the two inner most annuli that we neglect computing the colour gradient. For the rest of the samples this does not occur. Moreover, in these samples less than 5% of the galaxies have their half light radii within the first annuli considered in the calculation of colour gradients, $0.67'' < R50 < 1.0''$ (3rd annulus in the SDSS database).

Fig. A2 shows the distribution of colour gradients of galaxies with $b/a > 0.6$ from the *S20* sample, divided in four ranges of half light radii. The cut in ellipticity allows us to isolate the tendency of colour gradients with $R50$. The ranges of $R50$ have been defined

using as boundaries the outer radii of the 4th, 5th and 6th annuli in which the SDSS database provides averaged surface brightness measurements. Fig. A2 shows that the largest amount of galaxies in sample *S20* have their *R50* within the 5th surface brightness annuli. This is also the case when considering all galaxies, independently of their ellipticity and it also holds for galaxies within the sample *S20.5*, while for sample *S19* there is an even amount of galaxies with their *R50* in either the 5th or 6th annulus. As it was pointed out before, all galaxies in our samples have at least four surface brightness measurements, from the 3rd to the 6th annulus. Thus, except for the *S21* sample, when obtaining colour gradients we are taking into account surface brightness measurements both inside and outside *R50*. This point is essential for any robust conclusion about the behaviour of colour gradients.

Median colour gradients are steeper for higher values of *R50* (*arcsec*), for all the defined luminosity-threshold samples. In Fig. A2 the ranges of values we study are defined by half light radii values in *arcsec*. Therefore gradient values could be smeared out depending on the amount of light considered. To further explore this point, we have also studied the tendency of colour gradients when comparing galaxies with similar physical transverse radius, i.e., defining ranges of *R50* measured in $h^{-1}kpc$. Different amount of surface brightness annuli account for a different amount of light for galaxies with similar sizes at different distances. Thus, in this way galaxies with colour gradients extracted from different amount of annuli are included in the same range.

Independently of the galactic ellipticity, the same tendency found for *R50* (*arcsec*) applies when separating galaxies by their *R50* ($h^{-1}kpc$): the larger *R50* is, the steeper a colour gradient is likely to be. Galaxies within the *S20.5* sample have median ($g - i$) colour gradients: -0.036 , -0.048 , -0.061 , -0.080 for $R50(h^{-1}kpc) \leq 2$; $2 < R50(h^{-1}kpc) \leq 3$; $3 < R50(h^{-1}kpc) \leq 4$; $R50(h^{-1}kpc) > 4$, respectively. The same tendency for median values is found for galaxies within the *S19* and *S20* samples. In Fig. A3 we present the variation with $R50(h^{-1}kpc)$ of the ($g - i$) colour gradient and its error, for galaxies in *S20*. Median colour gradient values tend to decrease with larger half light radii, though, the correlation is dominated by the dispersion. When defining the colour gradient in decades of normalised radii (radius in logarithmic units), we also find that colour gradients get steeper for galaxies with larger *R50*. Tortora et al. (2010) finds a similar tendency with effective radius, supporting the robustness of our result.

Dividing our sample into late and early-types according to the concentration index, we found that the colour-gradient of late-type galaxies change more rapidly with the galactic size than early-types. The corresponding slopes for samples *S19*, *S20* and *S25* are: -0.028 , -0.025 and -0.024 for late-types and -0.004 , -0.002 and -0.002 for early-types galaxies. Colour gradient of early-type galaxies, remain quite constant with galactic size.

For the samples of galaxies under study, the colour gradient variation with *R50* has been found to be independent of the amount of light used for obtaining it. Still, the deeming of colour gradients could be partly due to calculating them with fewer annuli with surface brightness measurements. If this were the case, we will expect a correlation between the gradient error and *R50* (*arcsec*). However, no clear tendency is found, though the errors dispersion clearly decreases for larger *R50* (see Fig. A2). This tendency cannot explain alone the variation with *R50* seen for colour gradients. However, this consideration brings us to point out the unclear role that colour gradients could play in biasing global galactic properties obtained by extrapolating spectral characteristics from the SDSS galactic cores. In their studies, both Scodreggio (2001)

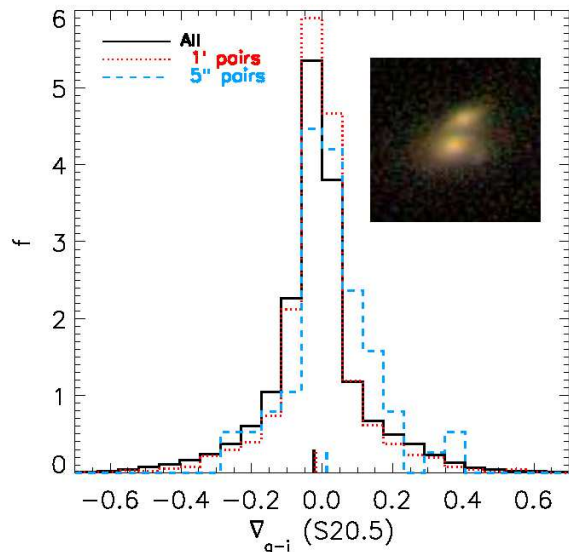


Figure A4. Distribution of ($g - i$) colour gradient for all the galaxies within *S20.5* sample, solid line, and for only close pairs of galaxies within either 1', dotted line, or 5'', dashed line, projected radius and 100 km/s in redshift. The inset shows an example of a pair of galaxies pair closer than 5'' projected radius. Histograms are normalised to give unit area underneath.

and Roche et al. (2009) found out that the colour gradients should be taken into account for estimating the evolution of the colour-magnitude relation in early-type galaxies.

Despite the large dispersion in colour gradients values, the results above suggest that on average, galaxies with larger *R50*, measured in either *arcsec* or *kpc*, intrinsically tend to have steeper colour gradients.

A3 Effect of having close pairs of galaxies on the colour gradient

Interacting galaxies can affect the colour gradients of each other. Moreover, colour gradient can be ill defined for close pairs of galaxies. Besides, the sky subtraction for close pairs of galaxies within the SDSS database may be problematic (John Lucey, private communication). Here we explore how the colour gradient distribute for close pairs of galaxies within our defined luminosity-threshold samples.

Fig. A4 show the distribution of colour gradients for galaxies that are within 100 km/s in redshift and within a projected radius of either 1' or 5''. This constitutes a lower limit to the fraction of close galactic pairs, since this number is expected to increase when including the whole photometric SDSS sample.⁷

We can observe that those close pairs with projected separations of maximum 1', present a distribution with a median value coincident with that of the total sample. These are only 5% of the total *S20.5* sample. Within the studied redshift range, 1' corresponds to around 100 kpc , approximately half the typical Virial radius of galaxies as massive as the Milky Way (Cooper et al. 2009). Thus,

⁷ SDSS could not observe galaxies closer than 55'' in the same plate and therefore close pairs are under represented in the spectroscopic sample. They were only observed in regions where spectroscopic plates overlapped.

this will be an approximate limit to find interacting pairs of galaxies, which could affect each other colour gradients. Since no clear bias is found we do not have any further reason to consider that the colour gradients of close pairs of galaxies as far as $1'$ apart is ill defined.

In the *S20.5* sample, we find 128 galaxies that are within 100 km/s in redshift and $5''$ projected from another galaxy. A visual inspection of these galaxies reveals pairs of interacting galaxies, with some of them showing clear tidal tails. However, most of these close pairs appear just as red double nucleated structures, similar to that shown in the inset of Fig. A4.

It is very interesting to see in Fig. A4 that these galaxies tend to present bluer cores than what expected from the total sample. This result could point out that the star formation triggered by galactic interactions could be responsible for the observed bluer cores. Simulation such as the one from Kobayashi (2004) suggest that this phase will decay with time into a flatter colour gradient. In any case, these galaxies represent a percentage far below 1% of the initial *S20.5* sample, and, therefore their contribution to increase the presence of blue nucleated galaxies is negligible at least in our sample.